



Contaminating Particle Movement in Insulating SF₆ Gas in Gas Insulated Switchgear (GIS)

Sherif Ghoneim, Ibrahim Bedir, Ahmed Alkhudaydi, Abdallah Alkhudaydi

Faculty of Engineering, Taif University-KSA

Abstract This paper focuses on the behavior of conduction particles motion in the insulating (Sulphurhexafluoride) SF₆ gas under the impulse voltage. These conducting particles play an important part on the reduction of the dielectric strength of the SF₆. The drag force based on the viscosity of insulating gas is taken into account. The effect of the particle shape, configuration of the gap, the atmosphere conditions and the dimensions of the contamination particles are investigated. The software program is carried out to simulate the motion of the contamination particles in insulating gas.

Keywords Sulphurhexafluoride (SF₆ gas), particle movement.

1. Introduction

SF₆ is a superior gas used as insulating medium in gas insulated system (GIS) and gas circuit breaker (GCB) [1-5]. Under specified conditions, the insulating gases have contaminated conducting particle. The origin of these particles may be generated from the manufacturing process, from mechanical vibrations or from moving parts of the system like circuit breakers or disconnectors etc. These particles may exist on the surface of support insulator, enclosure or high voltage conductor. The electrostatic forces can cause the contamination conducting particle to bounce into the high field region near the high voltage electrode; therefore a breakdown occurs making a short circuit of a part of insulation. These contaminated conduction particles can be therefore a problem with gas insulated substations operating at high fields [6-8]. The presence of the metallic particles in insulated gases will dramatically reduce the dielectric strength of it. This work focuses on the movement of contaminated conducting particles in insulating SF₆ gas. The movement of these conducting particles supports the breakdown occurrence because of carrying charges and approaching to the high voltage electrode. The effect of different configuration shapes of the gap, existence of the drag forces, shape of the particles, shape of applied impulse voltages, the atmospheric conditions and the particles dimension will be investigated.

2. Particle Movement under Impulse Voltage in GIS

Contaminating particles move randomly in GIS under electric field. This movement plays a crucial role in determining the insulation behavior. The micro-discharge and, in turn, the breakdown voltage, depends on particle shape, size, material, location and motion, gas pressure and nature of the applied field. Various authors in their attempt to gain an understanding of particle-initiated breakdown in SF₆ studied the effects of these parameters. This work examines the dynamics of free conducting particles in compressed SF₆ gas under applied impulse voltage.

A conducting particle, spherical or wire shape moving in compressed gas insulation would do so under the collective influence of the following forces as shown in Figure 1:



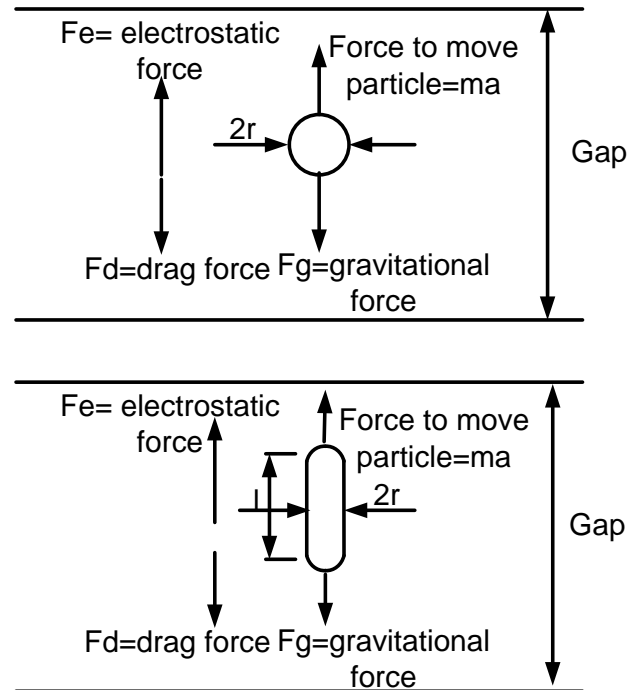


Figure 1: Forces affecting on the contaminated spherical and wire particles

- Electrostatic forces which are dependent on the local field, the charge on the particle and the local ionization activity, if any. This force may assist or oppose motion depending on the field direction and the polarity of the carried charge.
 - Gravitational force, which is a function of the particle's mass and affect downward.
- Drag force, which constantly opposes motion, is a function of particle velocity, gas viscosity and density and the particle shape and dimension [10].

The Equation of motion of a conducting particle carrying a charge (Q) in a compressed gas is:

$$m \ddot{X} = F_e(t) - F_d \pm F_g \quad (1)$$

where, \ddot{X} is the particle acceleration during motion, $F_e(t)$ is the electrostatic force ($F_e(t) = k_f Q \cdot E(t)$), $E(t)$ is the ambient field, k_f is a constant depending on particle shape and position, F_d is the drag force ($F_d = b_1 \dot{X}$), b_1 is in general a function of particle velocity (\dot{X}), F_g is gravitational force ($F_g = mg$), m is particle mass and g is gravitational acceleration.

3. Drag Force

The effect of gas pressure on particle motion can't be accounted for unless the drag force is considered. The drag forces on spherical and filamentary wire particles are examined in this section:

3.1. Drag force on spherical particles

Theoretically, for small relative velocities the drag force on a moving sphere (F_{d1}) is proportional to the velocity [11].

$$F_{d1} = 6 \pi \mu_v r \dot{X} \quad (2)$$

where, r is the particle radius (m), μ_v is the dynamic (absolute) viscosity of the fluid in (kg/m.sec), and (\dot{X}) is the velocity of the particle relative to the fluid in (m/sec).

Equation (2) is valid for a Reynolds numbers (R_e) less than about 5.

where,



$$R_e = \frac{2 \rho_g r \dot{X}}{\mu_v} \quad (3)$$

where, ρ_g is the gas density (kg/m^3). The viscosity (μ_v) is mainly a function of temperature. The gas density, meanwhile, is very much dependent on pressure. Typically, for SF_6 at 20 °C, raising the pressure from 0.1 to 1.0 MPa increases the density from about 14 to 90 (kg/m^3).

At higher Reynolds numbers, Equation (2) loses its linearity and is defined by;

$$F_{d1} = 6 \pi \mu_v r \dot{X} K_d \quad (4)$$

where, (K_d) is a coefficient which increases with (R_e) in a manner that is very closely expressed by;

$$K_d = e^{[0.1142 + 0.0543 \ln Re + 0.051(\ln Re)^2]} \quad (5)$$

for $5 < R_e < 1000$

3.2. Drag force on wire particles

A filamentary wire particle shaped as a longitudinal cylinder and hemi-spherically terminated at both ends and moving in a compressible fluid encounters two drag force components. The drag force on the two hemi-spherical ends (F_{d1}) which is equal to that on a sphere having the same radius as that of the wire and thus obeys relation (4) [12]. The second drag force on a wire particle is that on its sides and is given by [12]:

$$F_{d2} = 1.328(2\pi r \dot{X} \sqrt{\dot{X} \mu_v \rho_g L}) \quad (6)$$

where, L is the height of semi-ellipsoidal wire particle. Therefore, the total drag force is given by,

$$F_d = F_{d1} + F_{d2} \quad (7)$$

Therefore,

$$F_d = \dot{X} [\pi r(6 \mu_v K_d + 2.656 \sqrt{\dot{X} \mu_v \rho_g L})] \quad (8)$$

4. Determine the Trace of the Particle Movement under Impulse Voltage

4.1. Drag fully accounted

The Equation of motion of a conducting particle carrying a charge (Q) in a compressed gas is given by Equation (1). The ambient field $E(t)$ is proportional to the applied impulse voltage $V(t)$. The latter is assumed to be of a double exponential impulse form and given as,

$$V(t) = K_p (e^{-\alpha t} - e^{-\beta t}) \quad (9)$$

Where, K_p , α and β are constants relating to the waveshape and magnitude. Therefore, $E(t)$ can be written as,

$$E(t) = \frac{K_p}{X \ln \frac{r_o}{r_i}} (e^{-\alpha(t+t_L)} - e^{-\beta(t+t_L)}) \quad (10)$$

where, (t_L) is the lift off time, obtained by solving Equation (10) after replacing $V(t)$ by the lifting voltage V_L . For a coaxial cylinder configuration, an equivalent particle travel distance is given by, $[X \ln (r_o/r_i)]$ where, X is the distance from center of a coaxial cylinder, r_o and r_i are the outer and inner radii of coaxial system. Equation (1) now reduces to

$$\ddot{X} = H [e^{-\alpha(t+t_L)} - e^{-\beta(t+t_L)}] - b\dot{X} - g \quad (11)$$

where, b is the drag coefficient /mass parameter ($b=b_1/m$), for spherical particle: $b_1 = 6 \pi \mu_v r K_d$ and for wire particle:

$$b_1 = [\pi r(6 \mu_v K_d + 2.656 \sqrt{\dot{X} \mu_v \rho_g L})]$$

$H = K_c K_p Q / (m \cdot r_o \ln(r_o/r_i))$, m is the particle mass [$m = \rho (4/3\pi r^3 + \pi r^2 L)$], and ρ is the density of particle material in (kg/m^3), K_p is waveshape constant and K_c is the constant depends on the gap configuration.



Integrating Equation (11) gives the particle velocity [13].

$$\dot{X} = H \left[-\frac{1}{\alpha} e^{-\alpha(t+t_L)} + \frac{1}{\beta} e^{-\beta(t+t_L)} \right] - b\dot{X} - gt + C_1 \quad (12)$$

The constant C_1 is obtained by assuming the particle to lift off from rest, i.e. $X = 0$ at $t = 0$.

Thus

$$C_1 = H \left[\frac{1}{\alpha} e^{-\alpha t_L} - \frac{1}{\beta} e^{-\beta t_L} \right]$$

Equation (12) now has the form

$$\dot{X} + bX = \Phi(t) \quad (13)$$

That solution may be shown to be

$$Xe^{\int b dt} = \int \Phi(t) e^{\int b dt} dt + C_2 \quad (14)$$

and C_2 is obtained by letting $X(t=0) = 0$, i.e. Distance is measured from the initial position solving the above Equation in X gives,

$$X(t) = \frac{H}{\alpha(b-\alpha)} e^{-\alpha(t+t_L)} + \frac{H}{\beta(b-\beta)} e^{-\beta(t+t_L)} - g \left[\frac{t}{b} - \frac{1}{b^2} \right] + \frac{C_1}{b} + C_2 e^{-bt} \quad (15)$$

Where,

$$C_2 = \frac{H}{\alpha(b-\alpha)} e^{-\alpha t_L} - \frac{H}{\beta(b-\beta)} e^{-\beta t_L} - \frac{g}{b^2} - \frac{C_1}{b} \quad (16)$$

4.2. Drag coefficient constant

The solution of Equation 1 when the drag coefficient constant is as Equation 15 except the parameter K_d in Equation 5 will be 1.

4.3. Negligible drag

At very low pressures, or with low particle velocities, drag forces may have negligible values. In such cases the drag coefficient/mass parameter [b (sec^{-1})] may be set to zero in Equation 16. To avoid indefinite answers, substitution will have to be made after obtaining the limits of $X(t)$, as b tends to zero. This yields the drag-free travel as,

$$X(t) = H \left[\frac{1}{\alpha^2} e^{-\alpha(t+t_L)} - \frac{1}{\beta^2} e^{-\beta(t+t_L)} \right] - \frac{gt^2}{2} + C_1 t + C_2 \quad (17)$$

Where,

$$C_2 = -H \left[\frac{1}{\alpha^2} e^{-\alpha(t_L)} - \frac{1}{\beta^2} e^{-\beta(t_L)} \right] \quad (18)$$

5. Lifting Field and Charge of a Spherical Particle

A particle resting at the bottom of an electrode will be lifted, if a sufficiently high voltage is applied, when the electrostatic force exceeds the gravitational force. Lebedev et. al. [10] and Felici [14] have calculated

the charge accumulated and the lifting electrostatic force on spherical particles in contact with a plane in a uniform field.

A spherical conducting particle of radius r (m) lying on the bottom electrode (the outer electrode in a coaxial system) as shown in Figure 1 and subjected to a constant ambient field (E) sustains an electrostatic force ($F_e = K_f \cdot Q \cdot E$) where, E is the ambient field, Q is the particle charge and K_f is a correction constant which, for a spherical particle is equal to 0.832 [15,16]. The particle lifts off when the electrostatic force is equal to or greater than the weight of particle ($m \cdot g$) as shown in Figure 1, where, m is the particle mass and g is the gravitational acceleration. Felici demonstrated analytically that the charge acquired by the particle is given by [10, 14];

$$Q = \frac{2}{3} \pi^3 \epsilon_o r^2 E \quad (19)$$

To calculate the lifting field and lifting charge the weight of the particle is equated to the electrostatic force as shown in Figure 1,

$$m g = k_f Q_o E_o \quad (20)$$

For a spherical particle, the particle mass is (m) = $\frac{4}{3} \pi r^3 \rho$ where, ρ is the particle material density. Put m in Equation 20, hence,

$$\frac{4}{3} \rho g \pi r^3 = k_f Q_o E_o = k_f \left(\frac{Q_o}{E_o} \right) E_o^2 \quad (21)$$

But from Equation 19,

$$\frac{Q_o}{E_o} = \frac{2}{3} \pi^3 \epsilon_o r^2 \quad (22)$$

Substitute Equation 22 in 21,

$$E_o = 473.8 \sqrt{\frac{r \rho}{k_f}} \text{ kV/m} \quad (23)$$

By substituting E_o into Equation (22), the accumulated charge on a spherical particle at lift off is given by;

$$Q_o = 0.95 \times 10^{-4} \sqrt{r^5 \rho} \quad (24)$$

6. Lifting Field and Charge of a Filamentary Wire Particle

In practical compressed gas insulated apparatus most contaminating particles have been reported to be filamentary in shape [17-20]. A filamentary particle may be represented by a semi-ellipsoid [17, 19] for which Felici [10] had derived the carried charge (Q) and the electrostatic force when it is in contact with a plane in constant ambient field. Based on Felici's work and recalling that filamentary particles were experimentally reported to lift off the bottom electrode in vertical (longitudinal) direction [17], the carried charge and lifting field in this case is given by Equations as.

$$Q_o = \frac{\pi \epsilon L^2 E_o}{\ln \frac{2L}{r} - 1} \quad (25)$$

and

$$E_o = \left(\ln \frac{2L}{r} - 1 \right) \sqrt{\frac{r^2 \rho g}{\epsilon L \left[\ln \frac{2L}{r} - 0.5 \right]}} \quad (26)$$

where, L is the height of semi-ellipsoidal of wire particle and r is the radius of its base.



To calculate the lifting field (E_o) and charge carried by a vertical wire particle represented by a longitudinal cylinder hemi-spherically terminated at both ends.

7. Results and discussion

The software code using Matlab is used to simulate the motion equations of the contaminated particle. Figure 2 shows the flow chart of the Matlab code. The effect of different configuration shapes of the gap, existence of the drag forces, shape of the particles, shape of applied impulse voltages, the atmospheric conditions and the particles dimension will be investigated. The particle motion program scenario will be as follows:

1. Insertion of system data: particle shape, gape shape, waveform shape, gas mixture properties and environmental parameters.
2. Calculation of accumulated particle charge lifting electric field, lifting voltage and lifting time.
3. Insertion of the drag type: neglected drag, drag coefficient constant and drag fully accounted.
4. Calculation of the trajectory motion of the contamination particle.

Figures 3 to 5 show the effect of particle dimensions on the lifting charge (Q_o) and lifting field (E_o).

Figure 3 describes the relation between lifting charge to lifting field ratio and radius of the base of the wire particle, with different (L/r) ratio. It is seen that increases of base radius of the semi-ellipsoidal wire particle cause an increase in lifting charge to lifting field ratio. At the same particle radius an increase in (L/r) ratio causes an increase in lifting charge to lifting field ratio.

Figure 4 introduces the effect of wire particle geometry on the lifting field; at smaller L/r the lifting field is high.

Figure 5 shows the relation between the lifting charge and base particle radius at different (L/r). An increase of particle radius causes an increase in lifting charge.

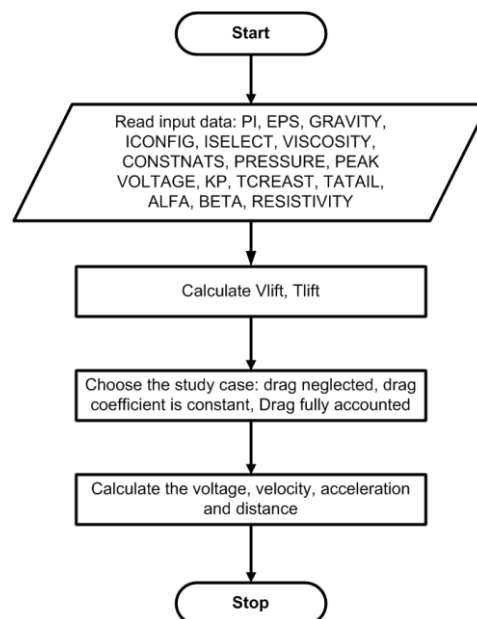


Figure 2: Flow chart of matlab code.



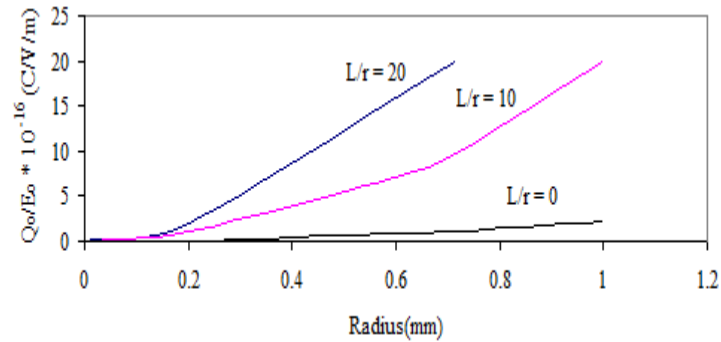


Figure 3: Effect of particle dimensions on the ratio of lifting charge per lifting field.

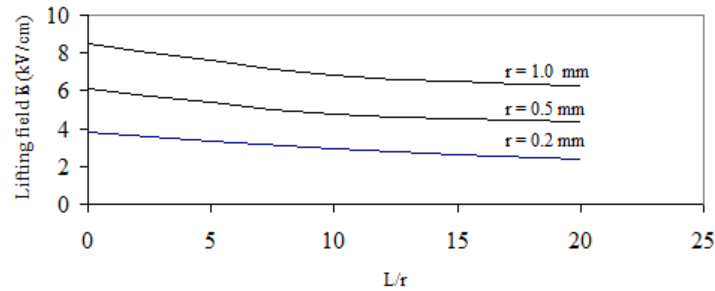


Figure 4: Effect of wire geometry on the lifting field.

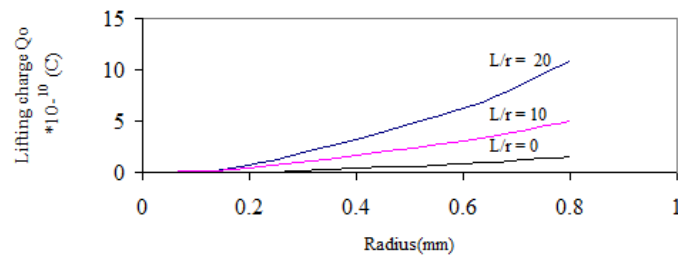


Figure 5: Effect of L/r on the lifting charge of the spherical and wire particle.

Figures 6 to 12 show the effect of particle dimensions and the applied impulse voltage on the movement of particle (spherical and filamentary wire) in GIS coaxial configuration as well as the effect of the pressure on the movement.

Figure 6 illustrates the relation between particle travel and the time at different peak values of applied impulse voltage for a spherical particle contaminating a coaxial cylinder. It is seen that an increase in applied impulse voltage cause an increase in electrostatic force and so an increase in distance travel by the particle. At the same applied impulse voltage the distance travel at negligible drag is more than that at drag fully accounted for.

Figure 7 describes the effect of spherical particle radius on the particle motion. When the particle radius is small then the particle is lighter and so crosses the gap faster.

Figure 8 illustrates the relation between particle travel and the time at different peak values of applied impulse voltage for a wire particle contaminating a coaxial cylinder. It is seen that an increase in time cause an increase of particle travel and at the same time an increase in applied impulse voltage cause an increase in electrostatic force and so an increase in distance travel by the particle. At the same applied impulse voltage the distance travel at negligible drag is more than that at drag fully accounted for.

Figure 9 studies the effect of height of semi-ellipsoidal wire particle (L) on its motion. It is seen that increases in height of semi-ellipsoidal wire particle (L) causes the particle crosses the gap faster.



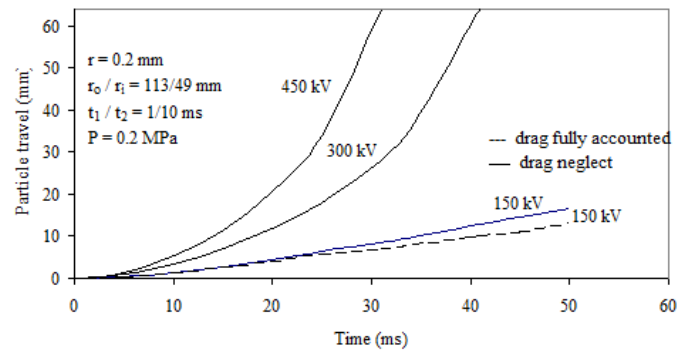


Fig. 6: Effect of applied impulse voltage on spherical particle trajectory contaminating SF6 coaxial gap.

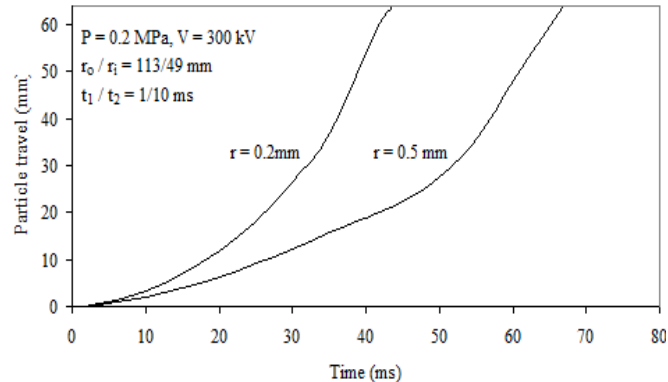


Figure 7: Effect of spherical particle radius on the movement of it in coaxial cylinder gap.

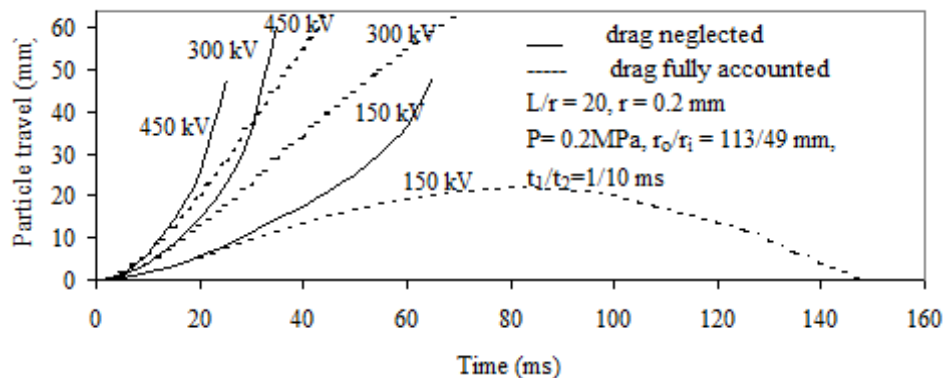


Figure 8: Effect of the applied impulse voltage on filamentary wire particle trajectory contaminating SF₆ coaxial gap.

Figure 10 describes the effect of wire particle radius on the particle motion. When the particle radius is small then the particle is lighter and so crosses the gap faster.

Figure 11 studies the effect of gas pressure on the movement. The Figure shows that when the drag is fully accounted for, the effect of gas pressure is significant. As shown in Figure 12 at 20 ms for example the displacement of the particle at this time in case of bar 1, bar 3, bar 5 and bar 7 is 8, 6.5, 6, 5.7 mm respectively. This means that when the pressure increase the particle will be slower.

8. Conclusions

- In this paper, a model has been formulated to simulate the movement of particle in different gas mixtures environment in gas insulated system (GIS). We have derived the exact formulas of the particle displacement, lifting voltage and lifting electric field for different contaminated particle configuration (spherical and wire) standing on a ground plane in a uniform electric field in pure SF₆ to study the dynamic behavior of these particles.

- The Equations of particle motion have been formulated and numerically solved when a contaminated metallic particle moves in different gap configurations such as parallel plane and coaxial cylinder gaps. Several dynamical phenomena have been investigated to illustrate the parameters that affect on the particle motion.
- The applied voltage plays an important role on the movement of the contaminated particle, an increase of the applied voltage the particle will be faster.

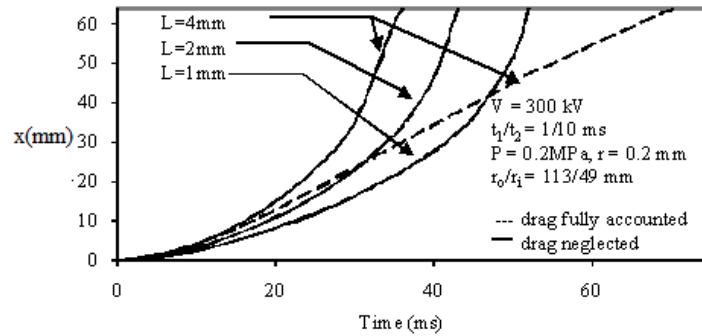


Figure 9: Effect of length of filamentary wire particle contamination through coaxial gap under applied impulse voltage.

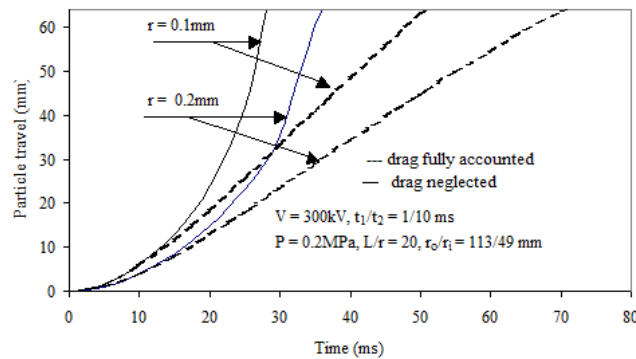


Figure 10: Effect of radius of filamentary wire particle on its motion through coaxial gap under applied impulse voltage.

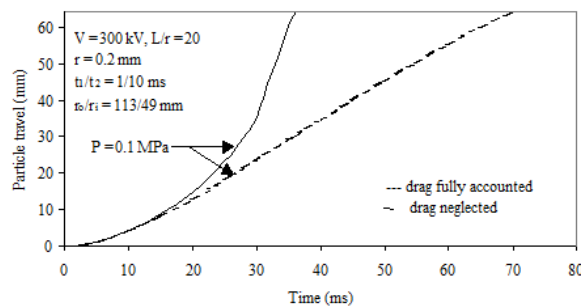


Figure 11: Effect of darg force on the motion of the contaminating particle.

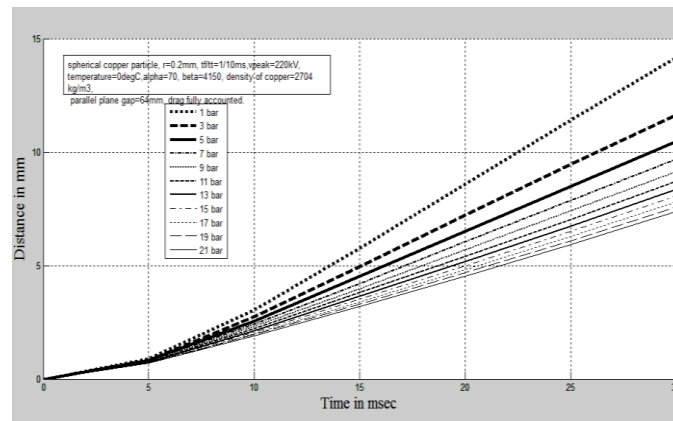


Figure 12: Effect of pressure on the movement of contaminated particle.

- The drag force impedes the movement of the contaminated particles, therefore, in case of drag fully accounted the motion of the particle is slower than that in case of drag neglect.
- In case of the spherical particle, when the particle radius increases, it means the volume of the particle and its weight increases, the movement of the particle will be reduced.
- In case of longitudinal (wire) particle, an increase of the particle length results in faster motion of the contaminated particle.
- An increase of the gas pressure will cause the viscosity increase and then, the gas impedes the motion of the contaminated particles.
- It is seen that increases of base radius of the semi-ellipsoidal wire particle cause an increase in lifting charge to lifting field ratio.
- At smaller L/r the lifting field is high.
- An increase of particle radius causes an increase in lifting charge.

References

1. Christophorou, L. G., & Van Brunt, R. J. (1995). SF_6/N_2 mixtures: basic and HV insulation properties. *Dielectrics and Electrical Insulation, IEEE Transactions on*, 2(5), 952-1003.
2. Okubo, H., & Hayakawa, N. (2004). Dielectric Characteristics and Electrical Insulation Design Techniques of Gases and Gas Mixtures as Alternatives to SF_6 . In *Gaseous Dielectrics X* (pp. 243-252). Springer US.
3. Takuma, T., Yamamoto, O., & Hamada, S. (2004). Gases as a dielectric. In *Gaseous Dielectrics X* (pp. 195-204). Springer US.
4. Hikita, M., Ohtsuka, S., Okabe, S., & Kaneko, S. (2008). Insulation characteristics of gas mixtures including perfluorocarbon gas. *Dielectrics and Electrical Insulation, IEEE Transactions on*, 15(4), 1015-1022.
5. Yamamoto, O., Takuma, T., Hamada, S., Yamakawa, Y., & Yashima, M. (2001). Applying a gas mixture containing $C-C_4F_8$ as an insulation medium. *Dielectrics and Electrical Insulation, IEEE Transactions on*, 8(6), 1075-1081.
6. Christophorou, L. G., & Van Brunt, R. J. (1995). SF_6/N_2 mixtures: basic and HV insulation properties. *Dielectrics and Electrical Insulation, IEEE Transactions on*, 2(5), 952-1003.
7. Morcos, M. M., Zhang, S., Srivastava, K. D., & Gubanski, S. M. (2000). Dynamics of metallic particle contaminants in GIS with dielectric-coated electrodes. *Power Delivery, IEEE Transactions on*, 15(2), 455-460.
8. Padmavathi, D., Amarnath, J., & Kamakshaiyah, S. (2009). Assesment of Dielectric Beaviour of SF_6/N_2 Gas Mixtures with Dielectric Coated Enclosure in a 1-Phase Gas Insulated Busduct in the Presence of Metallic Particle Contamination. Proceedings of the 16th International Symposium on High Voltage Engineering, Innes House, Johannesburg, South Africa, paper C-28, 2009.
9. Qiu, Y., & Feng, Y. P. (1996). June Investigation of S &- N_2 , SF_6-CO_2 and SF_6 -Air as Substitutes for SF_6 Insulation. In *Electrical Insulation, 1996., Conference Record of the 1996 IEEE International Symposium on* (Vol. 2, pp. 766-769). IEEE.
10. Lebedev, N. N., & Skalskaya, I. P. (1962). Force acting on a conducting sphere in field of a parallel plate condenser. *Soviet Physics-Technical Physics*, 7(3), 375-378.



11. Eskinazi, S. (1968). *Principles of fluid mechanics*. Allyn and Bacon, Inc., Boston, U.S.A.
12. Anis, H., & Srivastava, K. D. (1980). Movement of charged conducting particles under Impulse Voltages in Compressed Gases. In *IEEE Int. Conf. on Industrial Applications*, 80 ch 1575-0, 1048-1055, 1980.
13. Bujotzek, M., & Seeger, M. (2013). Parameter dependence of gaseous insulation in SF₆. *Dielectrics and Electrical Insulation, IEEE Transactions on*, 20(3), 845-855.
14. Felici, N. J. (1966). Forces et charges de petits objets en contact avec une électrode affectée d'un champ électrique. *Revue Générale de l'Électricité*, 75, 1145-60.
15. Anis, H., & Srivastava, K. D. (1981). Free conducting particles in compressed gas insulation. *Electrical Insulation, IEEE Transactions on*, (4), 327-338.
16. Anis, H., & Ward, S. (1988, October). Performance of coated GIS conductors under impulse voltages. In *Electrical Insulation and Dielectric Phenomena, 1988. Annual Report., Conference on* (pp. 312-317). IEEE.
17. Cookson, A. H., Bolin, P. C., Doepken, H. C., Wootton, R. E., Cooke, C. M., & Trump, J. G. (1976, August). Recent research in the United States on the effect of particle contamination reducing the breakdown voltage in compressed gas-insulated systems. In *Int. Conf. On Large High Voltage System*, CIGRE, Report No.15-09.
18. Cooke, C. M., Wootton, R. E., & Cookson, A. H. (1977). Influence of particles on AC and DC electrical performance of gas insulated systems at extra-high-voltage. *Power Apparatus and Systems, IEEE Transactions on*, 96(3), 768-777.
19. Cookson, A. H., & Wotton, R. E. (1975, September). Movement of filamentary conducting particles under AC voltages in high pressure gases. In *International Symposium Hochspannungstechnik Zurich*.
20. Latha, N. S., & Amarnath, J. (2013). Effect of Various Operating Parameters on Movement of Particle Contamination in Gas Insulated Substations. *International Journal of Scientific & Engineering Research*, 4(1), 1-5.
21. Bird, R. B., Stewart, W. E., & Lightfoot, E. N. Transport phenomena. 2002. 2nd Ed JohnWiley & Sons, New York.

